Jpn J Radiol (2017) 35:664–672
DOI 10.1007/s11604-017-0679-y

ORIGINAL ARTICLE

Involvement of miR-155/FOXO3a and miR-222/PTEN in acquired radioresistance of colorectal cancer cell line

Hamed Manoochehri Khoshinani[1] · Saeid Afshar[1] · Abdolazim Sedighi Pashaki[2] · Ali Mahdavinezhad[1] · Safora Nikzad[3] · Rezvan Najafi[1] · Razieh Amini[1] · Mohammad Hadi Gholami[2] · Alireza khoshghadam[2] · Massoud Saidijam[1]

Received: 19 May 2017 / Accepted: 16 August 2017 / Published online: 6 September 2017

Abstract
Purpose Finding a novel biomarker for determining the radiosensitivity of colorectal cancer (CRC) is critical. The aim of this study is to evaluate the role of two main miRNAs including miR-222 and miR-155 in radiation response of CRC.
Materials and methods The radioresistant CRC cell lines were established by exposing the HCT 116 cell line to fractional X-ray radiation. SubG1 fraction analysis, MTT and clonogenic assays were applied to evaluate acquired radioresistant cell line radiosensitivity. miR-222/PTEN and miR-155/FOXO3a expressions were detected by RT PCR.
Results The clonogenic assay and sub-G1fraction analysis indicated that the RR2 sub-line was significantly more resistant than the parental cell line. MiR-222 and miR-155 were significantly upregulated in the radioresistant cell lines compared with the parental cell lines. The PTEN and FOXO3a expressions in the radioresistant cell lines were significantly higher than in the parental line.
Conclusion These observations indicate that miR-222 and miR-155 could induce radiation resistance in colorectal cancer by targeting PTEN and FOXO3a genes, respectively. Therefore, miR-222 and miR-155 can be suggested as good biomarkers of CRC radiation response.

Keywords Colorectal neoplasms · Radioresistance · Radiation · miR-222 · miR-155

Introduction

The inherent or acquired radioresistance of colorectal tumors leads to failure of treatment and more toxic effects of ionizing radiation [1–4]. Using appropriate biomarkers of tumor radiosensitivity, we can predict the efficacy of radiotherapy and select a proper treatment strategy accordingly. There are several biomarkers, such as EGFR, p53, Bcl-2, Bax and p21, and several clinical factors that may be used as radiation response markers. However, the clinical application of these markers for the response of CRC to radiotherapy remains controversial and reliable identification of a patient's response to radiotherapy is still impossible [5–7].

Recent studies on the molecular biology of CRC indicate that the origin of radioresistance of CRC is related to tumor microenvironment and dysregulation of specific genes which play a critical role in cell signaling pathways. These genes are entitled oncogenes or tumor suppressors [8]. Furthermore, miRNAs as epigenetic factors play a key role in the pathogenesis of CRC [9, 10]. MicroRNAs (miRNAs) are small (18–24 nucleotide), noncoding RNA molecules that down-regulate their specific target genes through specific binding to the 3′-untranslated region (3′-UTR) of target mRNAs, suppressing mRNA translation or mRNA degradation [11].

Transcription of miRNA genes yields a primary miRNA (pri-miRNA). After processing of pri-miRNA by Drosha, pre-miRNA (about 70 nucleotides) is generated. Further

Hamed Manoochehri Khoshinani and Saeid Afshar contributed equally to this work.

✉ Massoud Saidijam
sjam110@yahoo.com

[1] Research Center for Molecular Medicine, Hamedan University of Medical Sciences, Hamadan, Iran

[2] Mahdieh Radiotherapy and Brachytherapy Charitable Center, Hamadan, Iran

[3] Department of Medical Physics, Hamadan University of Medical Sciences, Hamadan, Iran

processing of pre-miRNAs in cytoplasm leads to mature miRNA generation [12, 13]. One strand of mature miRNA specifically enters an RNA-induced silencing complex (RISC), then the activated RISC complex targets the target mRNA [14]. MiRNAs can control different biological functions including metabolism, autophagy, differentiation, inflammation, apoptosis and DNA damage response [15]. Based on the results of recent studies, miRNAs play a significant role in pathogenesis, prognosis, and progression of cancers [3, 11]. MiRNAs regulate the response of tumors to radiation through interaction with critical factors in PI3K/AKT, MAPK/ERK, NF-κB, or TGF-β pathways, which are essential radiation-related signal transduction pathways [15].

In summary, due to different responses of CRC patients to preoperative radiotherapy, and lack of a specific biomarker for distinguishing radiosensitive from radioresistant CRC tumors, identification and development of a novel biomarker of radiosensitivity are vital [16, 17]. On the other hand, considering the function of miRNAs in regulating the essential genes that determine tumor cells' radiosensitivity, we hypothesized that miRNA expression is different between radioresistant and radiosensitive CRC cell lines. Deregulation of miR-222 [18] (Gene ID: 407007) and miR-155 [19] (Gene ID: 406947) in several cancers and their dysregulation in response to radiation have been previously reported [20–25]. Therefore, the aim of this study was to investigate the expression changes of miR-222 and miR-155 and their candidate target genes in acquired radioresistant and parental radiosensitive colorectal cancer cell lines.

Materials and methods

Cell line and cell culture

The colorectal cancer cell line HCT 116 was purchased from the Pasteur Institute of Iran. The cell was cultured in high glucose DMEM medium (Gibco, USA), supplemented with 10% heat-inactivated fetal bovine serum (Gibco, USA) and 1% Pen-Strep (Gibco, USA) and incubated at 37 °C in a 5% CO_2 atmosphere with high relative humidity.

Establishing radioresistant cell lines

Radioresistant cell lines were established based on the method recommended by Su et al. [26]. The cells were fractionally irradiated by 6-MeV X-ray radiation with a high-energy linear accelerator (Shimva, China) at a dose rate of 200 MU per min (1 MU equals 1 cGy of absorbed dose in water under specific calibration conditions for the medical linear accelerator). The cells were first grown to 50% confluence in 25-cm^2 culture flasks. After irradiation with 1 Gy, the medium was changed immediately, and until 90% confluency, the cells were incubated at 37 °C. At 90% confluence, the adequate cells were sub-cultured into new flasks. When the new flask reached 50% confluence again, the cells were re-irradiated by 1 Gy (second fraction). These procedures were repeated 9 times (1 Gy 3 times, 2 Gy 3 times and 4 Gy 3 times) to a total dose of 21 Gy. When a radioresistant cell line with a total dose of 21 Gy was established, it was named a RR1 cell line. The RR1 sub-line was irradiated 4 more times with 6 Gy until a RR2 cell line with a total dose of 45 Gy was established. The parental cells underwent the same procedure under the same culture conditions, only without irradiation. Previous to all assays, radioresistant cells must be cultured without any intervention for at least 3 weeks after the last irradiation.

MicroRNA target genes prediction

The analysis of miR-222- and miR-155-predicted targets was performed using the following four algorithms: TargetScan (http://targetscan.org), miRanda (http://www.microrna.org/microrna/home.do), microT_CDS (http://diana.imis.athena-innovation.gr) and RNAhybrid (https://bibiserv2.cebitec.uni-bielefeld.de/rnahybrid).

In this study, the target genes were selected by considering their high prediction score and their confirmed role in cell cycle arrest or DNA damage repair and apoptosis signaling pathway.

Clonogenic assay (colony formation assay)

A clonogenic assay was applied to determine the radiosensitivity of each cell line. A predetermined number of viable cells, based on cell counting by trypan blue (900 cells for 0, 2 and 4 Gy, 1350 cells for 6 and 8 Gy), were seeded in 6-well culture plates and the plates were incubated at 37 °C for 24 h. The cells were irradiated with different doses of X-ray radiation (0, 2, 4, 6 and 8 Gy) and then incubated until the proper size of colonies was seen (10 days). The wells of the plate were then washed with PBS and stained with 0.5% crystal violet in 50% methanol. After washing and drying of plates, the colonies containing ≥ 50 cells were counted. Using the following formulas, the survival fractions (SF) were calculated, and the plating efficiency (PE) was calculated for cells which were not irradiated [27]. All tests were replicated 3 times.

$$\mathrm{PE} = \frac{\text{Number of colonies counted}}{\text{Number of cells seeded}} \times 100$$

$$\mathrm{SF} = \frac{\text{PE of irritated cells}}{\text{PE of control cells}} \times 100$$

After estimating the survival fraction at different radiation doses, the survival curve (log of survival fraction versus

radiation dose) was plotted and the D_0 value for each cell line was calculated using the following equation:

$$SF = 1 - \left(1 - e^{\frac{D}{D_0}}\right)^n$$

MTT assay

About 2×10^4 cells were seeded in 96-well plates at 100 µl/well. After 24 h of incubation at 37 °C, the cells were treated with a range of 6-MeV IR doses (0, 2, 4, 6 and 8 Gy). For a period of 144 to 192 h after irradiation, a linear relationship was observed between OD and number of live cells. An MTT assay was done following 168 h of irradiation. Briefly, 10 µl MTT solution [3-(4,5-dimethylthiazol-2-yl)-2,5-diphenyltetrazolium bromide solution, 5 mg/ml MTT] was added to each well and the plates were incubated at 37 °C for 4 h. Following the incubation, the solution from each well was removed and 100 µl of DMSO was added to each well to dissolve the formazan crystals. Plates were shaken for 15 min on a plate shaker to ensure adequate formazan solubility. The absorbance of the plate was read at 570 nm wavelength using an automatic microplate reader. The experiments were repeated 3 times. Finally, survival fraction was calculated by absorbance readings at 168 h after radiation using the following formula [27]:

$$SF = \frac{\text{Mean OD in test wells} - \text{Mean OD in cell free wells}}{\text{Mean OD in control wells} - \text{Mean OD in cell free wells}} \times 100$$

Sub-G1 fraction analysis

The fixation and staining of cells were done based on Pozarowski and Darzynkiewicz's method (with some modifications) [28]. In brief, around 3×10^5 of each cell line were seeded in 6-well culture plates and treated with 4 and 6 Gy X-ray radiation following 24 h of incubation at 37 °C. These cells were harvested after 48 and 72 h of radiation. They were then washed with PBS and fixed with 70% ethanol and stored at +4 °C for at least 2 h. After washing with PBS, the cells were resuspended in a solution containing 50 µg/ml of propidium iodide and 100 µg/ml of RNase A, followed by a 20-min incubation at 37 °C. The fluorescence in FL2 was collected by a Partec Flow cytometer.

RNA extraction

Total RNA was prepared using RNX™-plus reagent (Cinnagen, Iran) according to the manufacturer's instructions. The quality and integrity of the extracted RNA were verified by 1% gel electrophoresis. The concentration and purity of RNA were verified by optical density measurements (260/280 nm ratios).

Primer designing

Human gene-specific primers for PTEN, FOXO3a, and GAPDH (internal control) were designed using Allele ID software (version 6). The specificity of designed primer pairs was checked in NCBI primer blast. The resulting primers were as follows:

PTEN, forward: 5′AGTCCAGAGCCATT-T-CCATC3′;

PTEN, reverse: 5′GATAAATATAGGTCAAGT CTAAG-TCG3′;

FOXO3a, forward: 5′TGAGTGAGAGGCAATAGC ATAC3′;

FOXO3a, reverse: 5′AGCACCTATACAGCACCA T-A-A-C3′;

GAPDH, forward: 5′AAGGCTGTGGGCAAGGTCATC3′;

GAPDH, reverse: 5′ GCGT-C-A-A-A-GGTGG-AGGAGT GG3′. Hsa-miR-222-3p, hsa-miR-155-5p and U6 snRNA (internal control) primer sets were purchased from Exiqon.

cDNA synthesis

Complementary DNA (cDNA) for mRNA expression analysis was synthesized using a First Strand cDNA Synthesis Kit (Fermentas, K1631) in a total 20-µl reaction mixture, according to the manufacturer's recommendations. cDNA synthesis for miRNA expression analysis was performed using miRCURY LNA™ Universal RT cDNA Synthesis Kit (Exiqon, Cat. No 203301) according to the instructions provided with the kit.

Real-time PCR

All real-time PCR assays were carried out by the Roche LightCycler® 96 system. Firstly, real-time PCR efficiency for all reactions was calculated from the standard curves (log of the DNA concentration used vs the CT) using the following formula: $E = 10^{\left(\frac{-1}{\text{slope}}\right)} - 1$. The efficiency of all reactions was close to 100%. The mRNA expression levels were evaluated using gene-specific primer pairs mixed with a SYBR® Premix ExTaq™ II Kit (Takara, Cat. No RR820B) in a final volume of 20 µl according to the manufacturer's recommended protocol. The specificity of PCR products was confirmed by 1% gel electrophoresis, melting peak and dissociation curve analysis. To confirm the expected molecular weight (size of amplification product), sequencing was performed (Bioneer, Korea). The miRNA expression levels were measured using a microRNA LNA™ PCR primer set and ExiLENT SYBR® Green master mix, 2.5 ml (Exiqon, Cat. No 203403) in a final volume of 10 µl according to the manufacturer's instructions. Specificity of miRNA real-time PCR product was confirmed by melting peak and dissociation curve analysis. Each experiment was performed in triplicate. The

comparative Ct (cycle threshold) method was used to present real-time PCR data. Fold change of gene was calculated using the Eq. $2^{-\Delta\Delta Ct}$ [29]. All statistical tests were performed based on ΔCT [Ct (gene, sample)–Ct (gene, control)]. Also, graphs show ΔCT on the ordinate, which has a reverse relationship with gene expression level.

Statistical analysis

All values are expressed in mean ± standard deviation. Comparisons between groups were analyzed with one-way ANOVA, Tukey post hoc, and independent samples *t*-test. A Pearson test was done to investigate the correlation between quantitative parameters. $P < 0.05$ was considered statistically significant.

Results

Morphological change of HCT 116 cell line after radiation

As seen in Fig. 1, the parental HCT 116 cell line has regular fusiform cell morphology, while the established RR1 cell line shows irregular cell morphology with sharp protrusion and increased intracellular particles. The RR2 cell line has oval/round morphology, granular appearance with increased cell volume, and appendixes are lost.

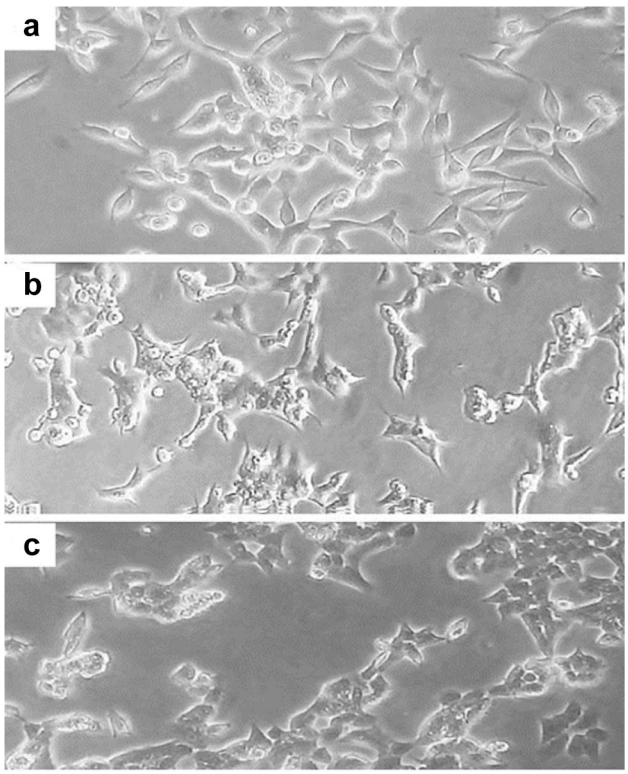

Fig. 1 Morphological comparison of RR2 (**c**), RR1 (**b**) and parental cell line (**a**). Parental cell line has a spindle form, RR1 cell line has cytoplasmic redundancy and RR2 cell line has a globular form

Evaluation of radiation sensitivity of colorectal cancer cell lines by colony formation assay

Radiosensitivities of the parental, RR1, and RR2 cell lines were investigated using a clonogenic assay. The D_0 (the dose that reduces the surviving fraction to 37%) of all cell lines are shown in Table 1. The D_0 was higher in the RR2 cell line than in the RR1 cell line. Furthermore, D_0 was higher in the RR1 cell line than in the parental cell line. Survival curves are shown in Fig. 2. SF2 (survival fraction at 2 Gy) of RR1, RR2, and parental cell lines were 61.75 ± 9.30, 58.16 ± 0.11, and 53.34 ± 1.38, respectively.

Survival fraction by MTT assay

The survival fractions of all cell lines at 2, 4, 6 and 8 Gy doses, were also calculated by MTT assay (168 h after radiation treatment). MTT survival fractions of all cell lines are compared in Fig. 3. It should be noted that the numerical value of MTT survival fraction was higher than the clonogenic survival fraction in all cell lines and

Table 1 D_0 dose value in RR2, RR1 and parental cell lines. RR2 cell line has higher D_0 value than RR1 and parental cell line

Cell lines	R^{2a}	D_0 (Gy)
RR2	0.9985	1.482
RR1	0.9997	1.340
Parental	0.9979	1.063

D_0 is a dose that reduces the surviving fraction to 37%

[a] R^2(R-squared) is the coefficient of determination for non-linear regression

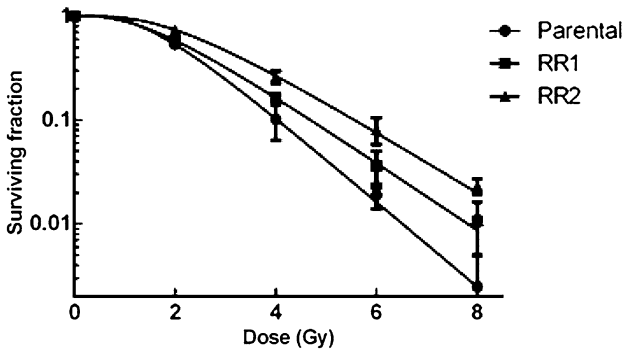

Fig. 2 Survival curve of RR2, RR1, and parental cell lines. Survival fraction of RR2 cell line is higher than RR1 and parental cell line at all doses

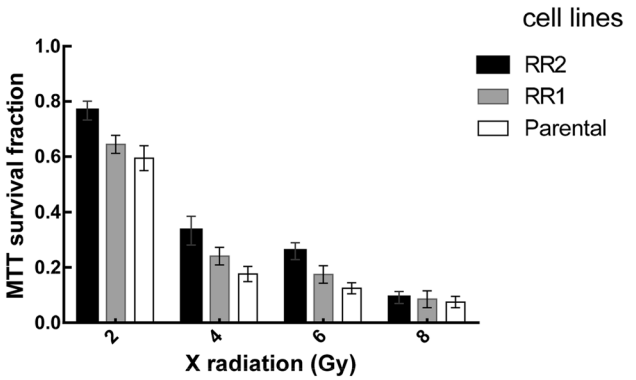

Fig. 3 MTT survival fraction versus radiation dose for all cell lines (168 h after radiation treatment). One-way ANOVA test showed a significant difference in survival fraction of three cell lines in 2-, 4- and 6-Gy doses. Tukey test results showed that MTT survival fraction of RR2 cell line at 2, 4 and 6 Gy was significantly larger than parental cell line. Survival fraction of RR1 cell line was significantly higher than parental cell line at 4 and 6 Gy

doses. However, the correlation between clonogenic and MTT assay was significant and linear (Pearson correlation = 0.991, *P* value = 0.00).

Sub-G1 fraction after radiation

In order to validate the radioresistance of the RR2 cell line, the sub-G1 fraction of parental and RR2 cell lines were evaluated and compared using the Partec Flow Max software. As seen in Fig. 4, the sub-G1 fraction of the parental cell line at 48 and 72 h following 4 Gy radiation and at 72 h after 6 Gy radiation was significantly higher than that of the RR2 cell line.

MiRNA target prediction results

Candidate genes were selected according to the following criteria: first, having a high prediction score at least in 3 of 4 databases; second, playing a role in cell radiation response (DNA damage response); and third, dysregulation in irradiated colorectal cancer cell lines. Four different prediction tools with different prediction algorithms were used for miRNA target evaluation. The *miTG* score. DIANA-*microT-CDS* is a weighted summation of the scores of all miRNA-recognition elements (MREs); the greater the MITG score is, the more probability of targeting is expected [30]. The TargetScan Total Context score predicts the relative repression of the mRNAs based on the targeting features such as site position, site number, site type, 3′-pairing contribution, and local AU content; a more negative score is interpreted as a better suppression [31]. The miranda-mirSVR score, which is a machine-learning method, evaluates the miRNA effect on the mRNA expression level; a more negative score means more suppression effect exists [32]. The RNAhybrid prediction tool was used for evaluating the minimum free energy (MFE) of miRNA and mRNA hybridization; a more negative MFE is a result of a more stable duplex [33].

Based on the above criteria, PTEN (Gene ID: 5728) and FOXO3a (Gene ID: 2309), which are important members of the phosphatidylinositol (PI)3-kinase pathway [18, 34], were selected as candidate target genes of miR-222 and miR-155 (respectively) for real-time PCR confirmation. Prediction scores for PTEN and FOXO3a as candidate target genes of miR-222 and miR-155 are shown in Table 2.

Real-time PCR analysis

There was no difference between mean CT values of GAPDH and U6 snRNA in the three cell lines (GAPDH *P* value = 0.210, U6 *P* value = 0.082). Therefore, they were suitable as reference genes to normalize gene expression between these cell lines.

A single peak was observed on the melting curve analysis, confirming the specificity of primers. Also, a single band of real-time PCR products on agarose gel was matched with PTEN and FOXO3a primer products length in NCBI primer blast. The sequencing data of real-time PCR products of FOXO3a and PTEN primers showed sequence similarity up to 99% with their mRNAs in NCBI/blast N.

MiR-222 was upregulated in RR2 and RR1 cell lines in comparison with the parental cell line, with an average increase of 2.03- and 2.48-fold, respectively. The expression level of miR-222 in RR2 (4.35 ± 0.26) and RR1 (4.06 ± 0.08) cell lines showed a statistically significant increase compared to parental cells (5.37 ± 0.24). However,

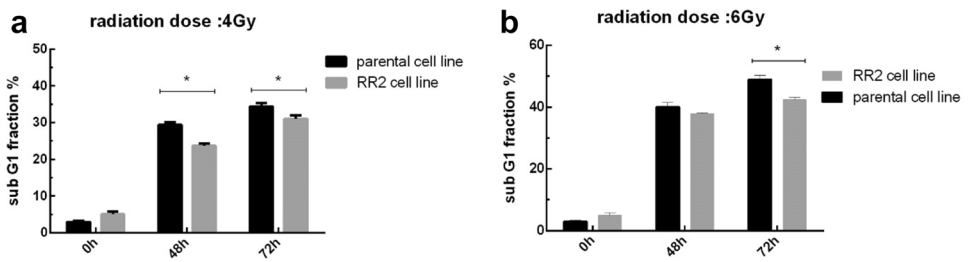

Fig. 4 Sub-G1 fraction of the parental and RR2 sub-line, following 4 Gy (**a**) and 6 Gy (**b**) radiation at indicated time point. **P* < 0.05 by independent sample *t*-test

Table 2 Different prediction score for miRNA target genes in a different database

	DIANA MicroT-CDS (miTG score)[a]	MiRanda (mirSVR score)[b]	TargetScan (total context score)[c]	RNAhybrid MFE[d]
miR-222, PTEN	0.811	−0.3829	−0.19	−27.9 kcal/mol
miR-155, FOXO3a	0.786	−0.193	−0.26	−26.5 kcal/mol

Four miRNA-mRNA interaction prediction tools, with different prediction algorithms, were used for miRNA target evaluation

[a] The greater the score, the more probability of targeting

[b] The more negative the score, the more suppression effect

[c] The more negative the score, the better suppression

[d] The more negative minimum free energy(MFE), the more stable the duplex is

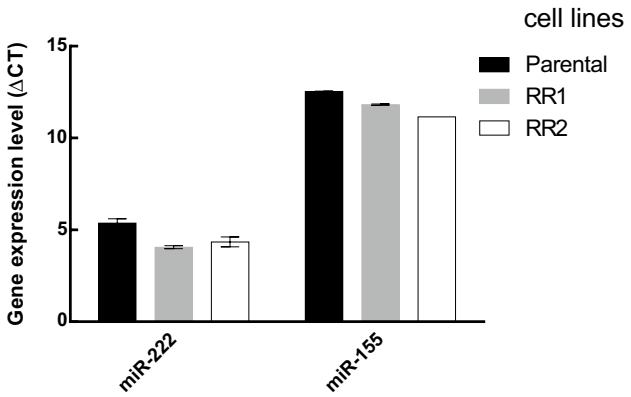

Fig. 5 MiR-222 and miR-155 expression levels. MiR-222 and miR-155 have a significantly higher expression in RR2 cell line in comparison to parental cell line. MiR-222 expression did not significantly change in RR2 cell line compared with RR1, while miR-155 was significantly overexpressed in RR2 cell line compared with RR1 cell line. The graph shows ΔCT which has a reverse relationship with gene expression level. $P < 0.05$ was considered to be a significant level by one-way ANOVA and Tukey post hoc tests

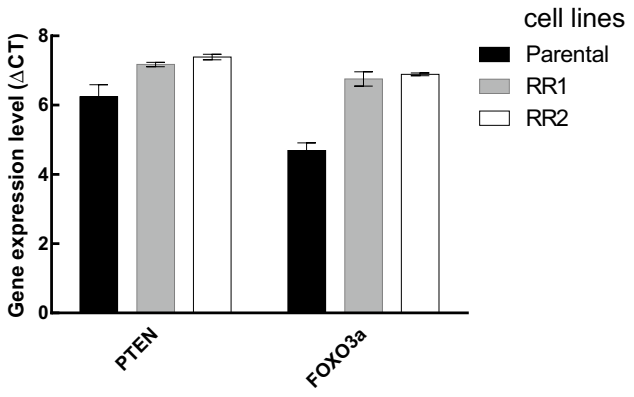

Fig. 6 PTEN and FOXO3a expression levels. PTEN and FOXO3a have a significantly lower expression in RR2 cell line in comparison to parental cell line. PTEN expression was significantly decreased in RR2 cell line compared with RR1 cell line. The expression level of FOXO3a was decreased in RR2 compared with RR1 cell line but this change wasn't statistically significant. The graph shows ΔCT which has a reverse relationship with gene expression level. $P < 0.05$ was considered to be a significant level by one-way ANOVA and Tukey post hoc tests

the expression level of miR-222 in RR1 and RR2 cell lines did not show a significant difference. The expression level of PTEN mRNA, a candidate target of miR-222, significantly decreased in RR2 (7.93 ± 0.08) and RR1 (7.17 ± 0.06) cell lines in comparison to the parental cell line (6.24 ± 0.34) with a fold change of −3.22 and −1.90, respectively. Also, PTEN expression in the RR2 cell line was significantly lower than the RR1 cell line (−1.69 fold) (Figs. 5, 6). ΔCt values of miR-222 and PTEN mRNA were compared with each other using the Pearson test. The results showed a significant negative correlation between miR-222 and PTEN expression (Pearson correlation = −0.866, P value = 0.026).

The miR-155 expression level was significantly increased in the RR2 and RR1 cell lines compared with the parental cell line, with a change of 2.58- and 1.64-fold, respectively. Also, miR-155 expression difference between RR1 and RR2 was significant with RR2 1.57 times greater than RR1. The expression level of FOXO3a mRNA, a candidate target of miR-155, was upregulated in RR2 and RR1 cell lines compared with the parental cell line with an average change of −4.59- and −4.16-fold, respectively. The expression levels of FOXO3a in RR1 and RR2 cell lines were not significantly different (Figs. 5, 6). There was a significant negative correlation between expression of miR-155 and FOXO3a gene (Pearson correlation = −0.889, P value = 0.025).

Discussion

In this study, we established radioresistant HCT 116 cell lines with repeated X-ray radiation. After comparing the radiosensitivities of the established cell lines and the parental cell line, a real-time PCR analysis was performed to examine the miR-222/PTEN and miR-155/FOXO3a expression.

The survival fraction at 2 Gy (SF2) and D_0 of the two cell lines (RR1 and RR2) after repeated irradiation were

significantly higher than the comparable values for the parental cell line. The results of the flow cytometry indicated that the sub-G1 fraction of the parental HCT 116 cell line after radiation was significantly higher than the RR2 cell line. Our results are in agreement with findings by Anastasov et al. [35] that showed apoptotic activity was significantly lower in radioresistant cell lines than in radiosensitive cell lines. Yang et al. [36] and Huang et al. [37] showed that D_0 and SF2 of HCT 116 as a radiosensitive cell line were about 0.8 Gy and 25%, respectively [36, 37]. On the other hand, D_0 and SF2 of SW-480 as an intrinsic radioresistant cell line were about 1.4 Gy and 60%, respectively. Results of another study [38] indicate that HCT 116 cells are significantly more sensitive to radiation (SF2 = 38.3%, D_0 = 2.23 Gy) when compared with HT-29 cells (SF2 = 61.4%, D_0 = 3.51 Gy). Results of our study indicate that radiosensitivity of RR1 and RR2 sub-lines such as intrinsic radioresistant cell lines (SW-480 and HT-29) were significantly lower than the parental HCT 116 cell line [37, 38]. However, the RR2 sub-line sustained a radioresistant phenotype for at least 3 months after termination of fractionated irradiation (data not shown).

MiR-222, as a well-recognized onco-miR, is frequently upregulated in several types of human tumors [39]. In our study, miR-222 was significantly upregulated in RR2 and RR1 cell lines compared with the parental cell line. In some studies [21, 22, 40], acute exposure to high dose ionizing radiation leads to up-regulation of miR-222. PTEN as a candidate target of miR-222 was significantly downregulated in RR2 and RR1 in comparison with the parental cell line and its expression showed a significant negative correlation with miR-222. PTEN functions as a tumor suppressor gene, specifically by negatively regulating the Akt/PKB signaling pathway. Reduced expression of PTEN results in Akt hyperactivation, thereby promoting cell proliferation, inhibition of apoptosis, and enhanced cell invasion and radioresistance [41–44]. So, we can postulate that miR-222 mediated radiation resistance of RR2 and RR1 cell lines by targeting PTEN via the PI3/Akt pathway. Although PTEN expression was significantly decreased in RR2 compared to the RR1 cell line, the expression level of miR-222 did not show a significant difference between the RR2 and RR1 cell lines. We assume other miRNAs (or other gene regulation systems) are involved in PTEN gene expression and PTEN has been suppressed by another miRNA in addition to miR-222. That hypothetical miRNA may be overexpressed in higher cumulative doses of X-radiation. According to some studies, one gene may be suppressed by several miRNAs [45, 46]. However, overall changes in PTEN expression level and miR-222 level between three cell lines were significant by one-way ANOVA test and a high and significant correlation was observed between miR-222 and PTEN.

MiR-155 as an onco-miR is over-expressed in various solid tumors [19, 47–49]. In this study, miR-155 expression was significantly increased in RR2 and RR1 cell lines compared with the parental cell line. Results of similar studies indicate that chronic and acute exposure irradiation lead to upregulation of miR-155 in cancerous cell lines [23, 24, 50, 51]. In our study, FOXO3a as a candidate target of miR-155, was significantly decreased in RR2 and RR1 cell lines in comparison with the parental cell line. Furthermore, a significant negative correlation between miR-155 and FOXO3a gene was observed. FOXO3a is a member of the forkhead family of transcription factors, which are downstream effectors of the PI3 K/PKB pathway and participate in a variety of cellular processes, such as cell cycle progression, programmed cell death, stress and DNA damage repair [52]. We can consider FOXO3a gene as a target of miR-155, and hence conclude that miR-155 leads to the radiation resistance of RR2 and RR1 cell lines by targeting FOXO3a via the PI3/Akt pathway. Although miR-155 expression level was significantly increased, the change in FOXO3a expression level between RR1 and RR2 was not significant. The explanation of this phenomenon is similar to miR-222/PTEN. It is also possible that miR-155 targets other genes in addition to FOXO3a. Furthermore, FOXO3a expression suppression mediated by miR-155 might have been compensated by downregulation of other miRNAs that target the FOXO3a gene. Based on the results of recent studies, one miRNA can suppress the expression of several target genes and each mRNA may be suppressed by several miRNAs [46, 53]. However, the one-way ANOVA revealed that the overall changes in miR-155 and FOXO3a expression level in the three cell lines were significant and there was a significant correlation between miR-155 and FOXO3a.

In previous studies, acquired radiation resistance of CRC has been explained by the following two mechanisms: first, adaptive response to fractional radiation, which leads to acquired radioresistance of tumor cells [37]; and second, radioresistance of tumor cells, which may originate from cancer stem cells (CSCs). Unlike CSCs, non-stem cancer cells are radiosensitive and will die under fractional radiation, thereby increasing the population of CSCs [54–59]. On the other hand, non-stem cancer cells can undergo dedifferentiation under fractional radiation, which induces generation of novel CSCs [60–62]. However, the mechanism of acquired radioresistance is outside the scope of the present study, and requires further investigation.

Conclusion

We have recognized that miR-222/PTEN and miR-155/FOXO3a mediate radiation resistance in colorectal cancer cell lines via the PI3/Akt pathway. After conducting the observational case–control study, in the future miR-222 and miR-155 can be used as novel biomarkers to predict

the effectiveness of radiotherapy in clinical cases. MiR-222 and miR-155 can also be used as clinical targets for reducing radiation resistance, although more accurate investigations such as using miRNA inhibition are needed. Finally, we suggest that cross-resistance of radioresistant sub-lines to different chemotherapeutic agents requires further evaluation.

Acknowledgements This study has been adapted from MSc and PhD theses at Hamadan University of Medical Sciences.

Compliance with ethical standards

Conflict of interest The authors declare that they have no conflict of interest.

Funding The study was funded by Vice-chancellor for Research and Technology, Hamadan University of Medical Sciences (Nos. 9412257365 and 9411136348).

References

1. Zhang Y, Zheng L, Huang J, Gao F, Lin X, He L, et al. MiR-124 radiosensitizes human colorectal cancer cells by targeting PRRX1. PLoS One. 2014;9(4):e93917.
2. Sandur SK, Deorukhkar A, Pandey MK, Pabón AM, Shentu S, Guha S, et al. Curcumin modulates the radiosensitivity of colorectal cancer cells by suppressing constitutive and inducible NF-κB activity. Int J Radiat Oncol Biol Phys. 2009;75(2):534–42.
3. Zheng L, Zhang Y, Liu Y, Zhou M, Lu Y, Yuan L, et al. MiR-106b induces cell radioresistance via the PTEN/PI3K/AKT pathways and p21 in colorectal cancer. J Transl Med. 2015;13(1):1.
4. Barker HE, Paget JT, Khan AA, Harrington KJ. The tumour microenvironment after radiotherapy: mechanisms of resistance and recurrence. Nat Rev Cancer. 2015;15(7):409–25.
5. Das P, Skibber JM, Rodriguez-Bigas MA, Feig BW, Chang GJ, Wolff RA, et al. Predictors of tumor response and downstaging in patients who receive preoperative chemoradiation for rectal cancer. Cancer. 2007;109(9):1750–5.
6. Kremser C, Trieb T, Rudisch A, Judmaier W, de Vries A. Dynamic T1 mapping predicts outcome of chemoradiation therapy in primary rectal carcinoma: sequence implementation and data analysis. J Magn Reson Imaging. 2007;26(3):662–71.
7. Jiang S, Wang R, Yu J, Zhu K, Mu D, Xu Z. Correlation of VEGF and Ki67 expression with sensitivity to neoadjuvant chemoradiation in rectal adenocarcinoma. Zhonghua zhong liu za zhi. 2008;30(8):602–5 **(Chinese Journal of Oncology)**.
8. Colibaseanu DT, Mathis KL, Abdelsatter ZM, Larson DW, Haddock MG, Dozois EJ. Is curative resection and long-term survival possible for locally re-recurrent colorectal cancer in the pelvis? Dis Colon Rectum. 2013;56(1):14–9.
9. Corté H, Manceau G, Blons H, Laurent-Puig P. MicroRNA and colorectal cancer. Dig Liver Dis. 2012;44(3):195–200.
10. Yang L, Belaguli N, Berger DH. MicroRNA and colorectal cancer. World J Surg. 2009;33(4):638–46.
11. Ma W, Yu J, Qi X, Liang L, Zhang Y, Ding Y, et al. Radiation-induced microRNA-622 causes radioresistance in colorectal cancer cells by down-regulating Rb. Oncotarget. 2015;6(18):15984.
12. Riffo-Campos ÁL, Riquelme I, Brebi-Mieville P. Tools for sequence-based miRNA target prediction: what to choose? Int J Mol Sci. 2016;17(12):1987.
13. Lin R-J, Lin Y-C, Chen J, Kuo H-H, Chen Y-Y, Diccianni MB, et al. MicroRNA signature and expression of Dicer and Drosha can predict prognosis and delineate risk groups in neuroblastoma. Cancer Res. 2010;70(20):7841–50.
14. MacFarlane L-A, Murphy RP. MicroRNA: biogenesis, function and role in cancer. Curr Genom. 2010;11(7):537–61.
15. Zhao L, Lu X, Cao Y. MicroRNA and signal transduction pathways in tumor radiation response. Cell Signal. 2013;25(7):1625–34.
16. Joye I, Haustermans K, editors. Which patients with rectal cancer do not need radiotherapy? Seminars in radiation oncology. Amsterdam: Elsevier; 2016.
17. Agostini M, Crotti S, Bedin C, Cecchin E, Maretto I, D'Angelo E, et al. Predictive response biomarkers in rectal cancer neoadjuvant treatment. Front Biosci. 2014;6:110–9.
18. Chun-zhi Z, Lei H, An-ling Z, Yan-chao F, Xiao Y, Guang-xiu W, et al. MicroRNA-221 and microRNA-222 regulate gastric carcinoma cell proliferation and radioresistance by targeting PTEN. BMC Cancer. 2010;10(1):1.
19. Jurkovicova D, Magyerkova M, Kulcsar L, Krivjanska M, Krivjansky V, Gibadulinova A, et al. MiR-155 as a diagnostic and prognostic marker in hematological and solid malignancies. Neoplasma. 2014;61(3):241–51.
20. Simone NL, Soule BP, Ly D, Saleh AD, Savage JE, DeGraff W, et al. Ionizing radiation-induced oxidative stress alters miRNA expression. PLoS One. 2009;4(7):e6377.
21. Templin T, Paul S, Amundson SA, Young EF, Barker CA, Wolden SL, et al. Radiation-induced micro-RNA expression changes in peripheral blood cells of radiotherapy patients. Int J Radiat Oncol Biol Phys. 2011;80(2):549–57.
22. Vincenti S, Brillante N, Lanza V, Bozzoni I, Presutti C, Chiani F, et al. HUVEC respond to radiation by inducing the expression of pro-angiogenic microRNAs. Radiat Res. 2011;175(5):535–46.
23. Chaudhry MA, Omaruddin RA, Kreger B, de Toledo SM, Azzam EI. Micro RNA responses to chronic or acute exposures to low dose ionizing radiation. Mol Biol Rep. 2012;39(7):7549–58.
24. Chaudhry MA, Sachdeva H, Omaruddin RA. Radiation-induced micro-RNA modulation in glioblastoma cells differing in DNA-repair pathways. DNA Cell Biol. 2010;29(9):553–61.
25. Gasparini P, Lovat F, Fassan M, Casadei L, Cascione L, Jacob NK, et al. Protective role of miR-155 in breast cancer through RAD51 targeting impairs homologous recombination after irradiation. Proc Natl Acad Sci. 2014;111(12):4536–41.
26. Su H, Jin X, Zhang X, Xue S, Deng X, Shen L, et al. Identification of microRNAs involved in the radioresistance of esophageal cancer cells. Cell Biol Int. 2014;38(3):318–25.
27. Nikzad S, Hashemi B. MTT assay instead of the clonogenic assay in measuring the response of cells to ionizing radiation. J Radiobiol. 2014;1(1):3–8.
28. Pozarowski P, Darzynkiewicz Z. Analysis of cell cycle by flow cytometry. Methods Mol Biol. 2004;281:301–11.
29. Livak KJ, Schmittgen TD. Analysis of relative gene expression data using real-time quantitative PCR and the $2^{-\Delta\Delta CT}$ method. Methods. 2001;25(4):402–8.
30. Riffo-Campos AL, Riquelme I, Brebi-Mieville P. Tools for sequence-based miRNA target prediction: What to choose? Int J Mol Sci. 2016;17(12):1987.
31. Garcia DM, Baek D, Shin C, Bell GW, Grimson A, Bartel DP. Weak seed-pairing stability and high target-site abundance decrease the proficiency of lsy-6 and other microRNAs. Nat Struct Mol Biol. 2011;18(10):1139–46.
32. Betel D, Koppal A, Agius P, Sander C, Leslie C. Comprehensive modeling of microRNA targets predicts functional non-conserved and non-canonical sites. Genome Biol. 2010;11(8):R90.

33. Rehmsmeier M, Steffen P, Hochsmann M, Giegerich R. Fast and effective prediction of microRNA/target duplexes. RNA. 2004;10(10):1507–17.
34. Essaghir A, Dif N, Marbehant CY, Coffer PJ, Demoulin J-B. The transcription of FOXO genes is stimulated by FOXO3 and repressed by growth factors. J Biol Chem. 2009;284(16):10334–42.
35. Anastasov N, Hofig I, Vasconcellos IG, Rappl K, Braselmann H, Ludyga N, et al. Radiation resistance due to high expression of miR-21 and G2/M checkpoint arrest in breast cancer cells. Radiat Oncol. 2012;7:206.
36. Yang XD, Xu XH, Zhang SY, Wu Y, Xing CG, Ru G, et al. Role of miR-100 in the radioresistance of colorectal cancer cells. Am J Cancer Res. 2015;5(2):545–59.
37. Huang MY, Wang JY, Chang HJ, Kuo CW, Tok TS, Lin SR. CDC25A, VAV1, TP73, BRCA1 and ZAP70 gene overexpression correlates with radiation response in colorectal cancer. Oncol Rep. 2011;25(5):1297–306.
38. Chendil D, Oakes R, Alcock RA, Patel N, Mayhew C, Mohiuddin M, et al. Low dose fractionated radiation enhances the radiosensitization effect of paclitaxel in colorectal tumor cells with mutant p53. Cancer. 2000;89(9):1893–900.
39. Matsuzaki J, Suzuki H. Role of microRNAs-221/222 in digestive systems. J Clin Med. 2015;4(8):1566–77.
40. Yang X-D, Xu X-H, Zhang S-Y, Wu Y, Xing C-G, Ru G, et al. Role of miR-100 in the radioresistance of colorectal cancer cells. Am J Cancer Res. 2015;5:545–59.
41. Ge H, Cao Y, Chen L, Wang Y, Chen Z, Wen D, et al. PTEN polymorphisms and the risk of esophageal carcinoma and gastric cardiac carcinoma in a high incidence region of China. Dis Esophagus. 2008;21(5):409–15.
42. Cinti C, Vindigni C, Zamparelli A, La Sala D, Epistolato MC, Marrelli D, et al. Activated Akt as an indicator of prognosis in gastric cancer. Virchows Arch. 2008;453(5):449–55.
43. Pappas G, Zumstein L, Munshi A, Hobbs M, Meyn R. Adenoviral-mediated PTEN expression radiosensitizes non-small cell lung cancer cells by suppressing DNA repair capacity. Cancer Gene Ther. 2007;14(6):543–9.
44. He XC, Yin T, Grindley JC, Tian Q, Sato T, Tao WA, et al. PTEN-deficient intestinal stem cells initiate intestinal polyposis. Nat Genet. 2007;39(2):189–98.
45. Qiao Y, Badduke C, Mercier E, Lewis SM, Pavlidis P, Rajcan-Separovic E. miRNA and miRNA target genes in copy number variations occurring in individuals with intellectual disability. BMC Genom. 2013;14(1):544.
46. Miranda KC, Huynh T, Tay Y, Ang Y-S, Tam W-L, Thomson AM, et al. A pattern-based method for the identification of microRNA binding sites and their corresponding heteroduplexes. Cell. 2006;126(6):1203–17.
47. Gironella M, Seux M, Xie M-J, Cano C, Tomasini R, Gommeaux J, et al. Tumor protein 53-induced nuclear protein 1 expression is repressed by miR-155, and its restoration inhibits pancreatic tumor development. Proc Natl Acad Sci. 2007;104(41):16170–5.
48. Iorio MV, Ferracin M, Liu C-G, Veronese A, Spizzo R, Sabbioni S, et al. MicroRNA gene expression deregulation in human breast cancer. Cancer Res. 2005;65(16):7065–70.
49. Yanaihara N, Caplen N, Bowman E, Seike M, Kumamoto K, Yi M, et al. Unique microRNA molecular profiles in lung cancer diagnosis and prognosis. Cancer Cell. 2006;9(3):189–98.
50. Chaudhry MA, Kreger B, Omaruddin RA. Transcriptional modulation of micro-RNA in human cells differing in radiation sensitivity. Int J Radiat Biol. 2010;86(7):569–83.
51. Chaudhry MA, Omaruddin RA, Brumbaugh CD, Tariq MA, Pourmand N. Identification of radiation-induced microRNA transcriptome by next-generation massively parallel sequencing. J Radiat Res. 2013;54(5):808–22.
52. de Mattos SF, Villalonga P, Clardy J, Lam EW. FOXO3a mediates the cytotoxic effects of cisplatin in colon cancer cells. Mol Cancer Ther. 2008;7(10):3237–46.
53. Lewis BP, Burge CB, Bartel DP. Conserved seed pairing, often flanked by adenosines, indicates that thousands of human genes are microRNA targets. Cell. 2005;120(1):15–20.
54. Reya T, Morrison SJ, Clarke MF, Weissman IL. Stem cells, cancer, and cancer stem cells. Nature. 2001;414(6859):105–11.
55. Civenni G, Walter A, Kobert N, Mihic-Probst D, Zipser M, Belloni B, et al. Human CD271-positive melanoma stem cells associated with metastasis establish tumor heterogeneity and long-term growth. Cancer Res. 2011;71(8):3098–109.
56. Bao S, Wu Q, McLendon RE, Hao Y, Shi Q, Hjelmeland AB, et al. Glioma stem cells promote radioresistance by preferential activation of the DNA damage response. Nature. 2006;444(7120):756–60.
57. Diehn M, Cho RW, Lobo NA, Kalisky T, Dorie MJ, Kulp AN, et al. Association of reactive oxygen species levels and radioresistance in cancer stem cells. Nature. 2009;458(7239):780–3.
58. Oravecz-Wilson KI, Philips ST, Yilmaz ÖH, Ames HM, Li L, Crawford BD, et al. Persistence of leukemia-initiating cells in a conditional knockin model of an imatinib-responsive myeloproliferative disorder. Cancer Cell. 2009;16(2):137–48.
59. Zhao C, Chen A, Jamieson CH, Fereshteh M, Abrahamsson A, Blum J, et al. Hedgehog signalling is essential for maintenance of cancer stem cells in myeloid leukaemia. Nature. 2009;458(7239):776–9.
60. Mani SA, Guo W, Liao M-J, Eaton EN, Ayyanan A, Zhou AY, et al. The epithelial-mesenchymal transition generates cells with properties of stem cells. Cell. 2008;133(4):704–15.
61. Chang L, Graham PH, Hao J, Bucci J, Cozzi PJ, Kearsley JH, et al. Emerging roles of radioresistance in prostate cancer metastasis and radiation therapy. Cancer Metastasis Rev. 2014;33(2–3):469–96.
62. Lagadec C, Vlashi E, Della Donna L, Dekmezian C, Pajonk F. Radiation-induced reprogramming of breast cancer cells. Stem Cells. 2012;30(5):833–44.